INSTITUTE OF PHYSICS PUBLISHING JOURNAL OF PHYSICS B: ATOMIC, MOLECULAR AND OPTICAL PHYSICS

J. Phys. B: At. Mol. Opt. Phys. **36** (2003) 1615–1626 PII: S0953-4075(03)59181-7

Electron collisions with ethylene

R Panajotovic[1], M Kitajima[2], H Tanaka[2], M Jelisavcic[1], J Lower[1], L Campbell[3], M J Brunger[3] and S J Buckman[1]

[1] Research School of Physical Sciences and Engineering, Australian National University, Canberra, ACT, Australia
[2] Physics Department, Sophia University, Chiyoda-ku, Tokyo, Japan
[3] School of Chemistry, Physics and Earth Sciences, Flinders University, GPO Box 2100, Adelaide, South Australia, Australia

Received 31 January 2003, in final form 7 March 2003
Published 3 April 2003
Online at stacks.iop.org/JPhysB/36/1615

Abstract

We have measured absolute elastic scattering and vibrational excitation cross sections for electron impact on ethylene. The experimental data have been obtained on two different crossed-beam electron spectrometers and they cover the energy range from 1 to 100 eV and scattering angles between 10° and 130°. Both differential (in angle) and energy-dependent cross sections have been measured. The differential cross sections have also been analysed using a molecular phase shift analysis technique in order to derive the integral elastic and elastic momentum transfer cross sections. Comparison is made with earlier data, where available, and also with a number of recent theoretical calculations.

1. Introduction

Despite being one of the simpler hydrocarbon molecules, ethylene or ethene (C_2H_4) has not been the subject of a great deal of study regarding either the dynamics or the magnitude of its interactions with low-energy electrons. In particular, the measurement of a comprehensive set of *absolute* scattering cross sections, and the detailed comparison of these with current theory, is somewhat lacking. Such cross sections, and their comparisons, are not only important for the further development of electron–polyatomic molecule scattering theory, but they are also of relevance to research in gas-discharge modelling, particularly in the way that they may help assess the accuracy of theoretical approaches to the calculation of cross sections for fluorinated hydrocarbons.

Previous studies which have provided information on low-energy electron collision cross sections for ethylene, and which are of relevance to the present work, include the elastic scattering measurements of Mapstone and Newell (1992), the vibrational excitation studies of Walker *et al* (1978), Lunt *et al* (1994) and Mapstone *et al* (2000) and the total cross section measurements of Floeder *et al* (1985), Sueoka and Mori (1986) and Lunt *et al* (1994). For the differential scattering studies, only a few of the cross section measurements are absolute

and those that are have either large uncertainties or were normalized in some fashion to obtain the absolute scale. The measurements of Walker *et al* showed that vibrational excitation of C_2H_4 is dominated by shape resonances of $^2B_{2g}$ (∼1.8 eV) and ^2A_g (∼7.5 eV) symmetries. Theoretical studies are even more limited, with the published work consisting of the Kohn variational calculations of Schneider *et al* (1991) and the Schwinger variational calculations of Winstead *et al* (1991), Brescansin *et al* (1998) and, most recently, Winstead and McKoy (2002). Most of this theoretical work has focused on the calculation of elastic scattering cross sections and, to our knowledge, there are no calculations for the vibrational excitation of C_2H_4.

Thus the main objective of the present work was to provide a body of absolute scattering cross sections for elastic scattering and vibrational excitation against which current theoretical efforts could be assessed. We present elastic scattering differential cross sections (DCS), which have been measured at a number of energies between 1 and 100 eV; elastic excitation functions (EFs) at a number of fixed angles for energies between 1 and 10 eV, and DCS for the excitation of a number of composite vibrational modes at an incident energy of 7.5 eV. We have also integrated the DCS to obtain integral elastic (ICS) and elastic momentum transfer cross sections (MTCS). These data are compared with other recent measurements and, where possible, with calculations from a number of different theoretical approaches. A preliminary report of some aspects of this work has appeared elsewhere (Panajotovic *et al* 2003).

2. Experimental apparatus and procedures

The scattering apparatus that has been used in both laboratories consists of conventional crossed-beam spectrometers. The details of the construction and operation of these spectrometers have been provided in a number of previous, joint publications (Kitajima *et al* (2000) and references therein and Cho *et al* (2001) and references therein) and we do not repeat them here. In both cases the absolute electron energy scale has been determined by measurements of resonance structures in N_2 (the low-lying $^2\Pi_g$ resonance) or He (the $1s2s^2\ ^2S$ resonance). The absolute scale for the cross sections is obtained by measuring scattering intensities for C_2H_4 relative to those for helium elastic scattering under experimental conditions which provide for identical scattering geometry for both measurements. The relative flow technique is applied in both cases and this has been described in great detail in previous papers from our laboratories. The helium cross sections which are used for the normalization are those of Nesbet (1979) or the recommended set of Boesten and Tanaka (1992). At the Australian National University (ANU) the target beams are formed by flowing the gases concerned through a 1 mm diameter capillary tube, which is 18.5 mm in length. Gas driving pressures of typically 0.1 Torr for C_2H_4 and 0.5 Torr for He are used. The measurements at Sophia (Sophia University, Japan), conducted using a 5 mm long capillary of internal diameter 0.3 mm, use a similar pressure ratio but operate at higher absolute pressures, 0.5 and 2.5 Torr respectively. The pressure ratios in each case are based on the requirement that the mean free paths for the two gases are identical in the beam-forming tube. The mean free paths were calculated from values of the hard-sphere diameters of 4.94 Å for C_2H_4 and 2.19 Å for He (Landolt-Börnstein 1971).

3. Results and discussion

3.1. Elastic scattering

Absolute DCSs for elastic electron scattering from ethylene molecules at energies between 1 and 100 eV are presented in table 1 and some examples are shown in figures 1 and 2, where comparison is made with earlier data and recent calculations. The uncertainty on the cross

Table 1. Elastic scattering cross sections, in units of 10^{-16} cm^2 sr^{-1}, for electron collisions with C_2H_4. Both the ANU (A) and Sophia (S) measurements are listed. For the ANU results the absolute uncertainty, expressed as a percentage, is given in parentheses. The uncertainty on the Sophia data is ±15%. The integral elastic cross sections (ICS) and elastic momentum transfer cross sections (MTCS) are given at the foot of each column in units of 10^{-16} cm^2. The uncertainty in these values is estimated to be 20–25%.

	Energy (eV)						
Angle	1.0 (A)	1.5 (S)	1.8 (S)	2.0 (A)	2.0 (S)	2.2 (S)	
20		0.581	1.26	2.48 (24)	1.66	1.34	
30	0.246 (50)	0.705	1.42	1.84 (19)	1.62	1.40	
40	0.294 (29)	0.667	1.30	1.71 (15)	1.55	1.45	
50	0.505 (18)	0.787	1.29	1.64 (15)	1.72	1.56	
60	0.878 (11)	1.04	1.28	1.70 (11)	1.79	1.55	
70	1.02 (9)	1.60	1.68	1.78 (9)	1.82	1.57	
80	1.23 (10)	1.92	1.99	1.84 (10)	1.88	1.86	
90	1.13 (16)	2.04	1.95	1.77 (11)	1.94	1.68	
100	1.30 (11)	1.90	1.83	1.55 (12)	1.82	1.57	
110	1.19 (15)	1.73	1.41	1.41 (10)	1.69	1.42	
120	1.06 (9)	1.39	1.36	1.43 (17)	1.52	1.37	
130	1.01 (15)	1.12	1.25	1.45 (16)	1.51	1.47	
ICS	12.7	16.3	18.4	21.87	21.3	19.4	
MTCS	15.2	16.8	17.9	21.15	20.8	19.3	
	2.5 (S)	3.0 (A)	3.1 (S)	4.1 (S)	4.5 (A)	4.6 (S)	5.0 (A)
15			1.79	2.59		3.26	3.79(11)
20	1.11	1.85(13)	1.77	2.44	2.76(12)	2.95	3.34(9)
25		1.74(8)			2.26(12)		—
30	1.32	1.64(9)	1.82	2.01	2.09(13)	2.31	2.37(10)
35		1.72(7)			2.08(10)		—
40	1.65	1.69(10)	1.94	1.94	2.06(9)	2.28	2.13(8)
45		1.77(8)	2.12		1.98(9)	2.36	—
50	1.78		2.24	2.09	1.93(9)	2.39	2.06(8)
55		1.71(8)	2.18			2.34	—
60	1.81	1.71(9)	2.09	2.18	1.71(8)	2.23	1.65(7)
70	1.90	1.51(8)	1.87	1.97	1.38(8)	1.96	1.31(7)
80	1.72	1.30(8)	1.81	1.75	1.07(8)	1.56	0.97(7)
90	1.59	1.15(8)	1.55	1.38	0.948(7)	1.35	0.832(8)
100	1.49	1.02(8)	1.33	1.15	0.895(8)	1.15	0.800(8)
110	1.46	0.970(8)	1.20	1.17	0.932(10)	1.19	0.877(8)
120	1.31	0.994(9)	1.09	1.04	0.985(8)	1.24	0.956(7)
130	1.36	1.10(9)	1.11	1.06	1.20(10)	1.30	1.10(8)
ICS	18.6	16.3	19.5	18.2	17.0	20.1	17.0
MTCS	17.6	14.3	17.3	14.6	14.0	16.3	13.3
	5.1 (S)	6.0 (A)	7.5 (A)	8.0 (A)	8.1 (S)	10.1 (S)	
15	6.05	6.09(12)	—	—	9.95	12.16	
20	4.54	4.66(8)	7.15(8)	8.43	8.39	9.47	
25		3.97(10)	—	6.54			
30	2.90	3.05(9)	4.27(10)	5.01	4.87	5.63	
35		—	—	4.05			
40	2.36	2.44(8)	2.81(9)	3.21	3.09	3.26	
45		—	—	2.66			
50	2.28	2.09(9)	2.19(10)	2.34	2.23	2.04	

Table 1. (Continued.)

	Energy (eV)						
Angle	5.1 (S)	6.0 (A)	7.5 (A)	8.0 (A)	8.1 (S)	10.1 (S)	
55		—	—	2.02			
60	2.27	1.73(8)	1.69(9)	1.60	1.70	1.48	
70	2.05	1.24(8)	1.17(8)	1.15	1.29	1.09	
80	1.51	0.872(8)	0.803(8)	0.791	1.01	0.849	
85				0.749			
90	1.21	0.744(7)	0.736(9)	0.766	0.898	0.677	
100	1.11	0.846(10)	1.02(9)	0.963	0.986	0.898	
110	1.14	1.06(8)	1.24(10)	1.21	1.17	1.02	
120	1.18	1.23(8)	1.59(9)	1.40	1.42	1.08	
130	1.35	1.31(8)	1.60(8)	1.43	1.35	1.04	
ICS	22.9	19.2	22.2	23.2	25.6	24.5	
MTCS	18.5	14.2	15.0	14.1	19.6	15.8	
Angle	15 (A)	15 (S)	20 (A)	20 (S)	30 (S)	60 (S)	100 (S)
10	20.92(9)		20.83(10)				
15	14.75(8)		14.15(7)				
20	11.27(8)	9.98	9.40(9)	9.47	7.40	3.20	2.02
25	7.68(9)		6.86(7)				
30	5.29(9)	5.40	4.10(7)	4.22	2.90	0.950	0.662
35	3.49(8)		2.75(7)				
40	2.37(7)	2.45	1.74(7)	1.95	1.20	0.525	0.310
45	1.69(8)		1.31(8)				
50	1.25(8)	1.32	0.981(10)	1.05	0.773	0.274	0.197
55	1.02(8)		0.774(8)				
60	0.799(8)	0.914	0.624(9)	0.713	0.531	0.197	0.153
70	0.592(8)	0.707	0.461(10)	0.597	0.351	0.158	0.099
80	0.446(8)	0.567	0.359(11)	0.438	0.277	0.118	0.074
90	0.446(8)	0.544	0.334(11)	0.426	0.256	0.108	0.069
100	0.544(7)	0.648	0.381(10)	0.454	0.264	0.113	0.070
110	0.623(8)	0.769	0.418(11)	0.477	0.311	0.114	0.079
120	0.671(8)	0.908	0.470(11)	0.559	0.332	0.131	0.086
130	0.716(8)	0.913	0.593(11)	0.563	0.392	0.178	0.103
ICS	23.6	22.8	19.5	18.5	12.3	6.14	3.73
MTCS	15.6	13.8	11.5	9.8	5.3	2.5	1.5

sections ranges between 6 and 15%, depending on the angle and energy and the source of the measurement. The uncertainties, expressed as a percentage, are indicated in the table.

The elastic cross sections for energies below 5 eV are shown in figure 1. At 1 eV (figure 1(a)) the present data are the first measurement of the elastic DCS at this energy. The cross section drops considerably towards small scattering angles and has a maximum value of just over 1 $Å^2$ sr^{-1} at around 100°. We compare the experimental results in this figure with the calculated cross sections from the Schwinger variational iterative method (SVIM) of Brescansin *et al* (1998) and cross sections calculated with the Kohn variational technique (Schneider *et al* 1991, Rescigno 2002). The SVIM calculation shows remarkably good agreement with the experiment for such a low energy. At 2 eV (figure 1(b)), an energy which is close to the peak of the low-lying $^2B_{2g}$ shape resonance (∼1.8 eV), the form of the cross section has changed considerably. The DCS is everywhere larger than at 1 eV and, although there is some shallow

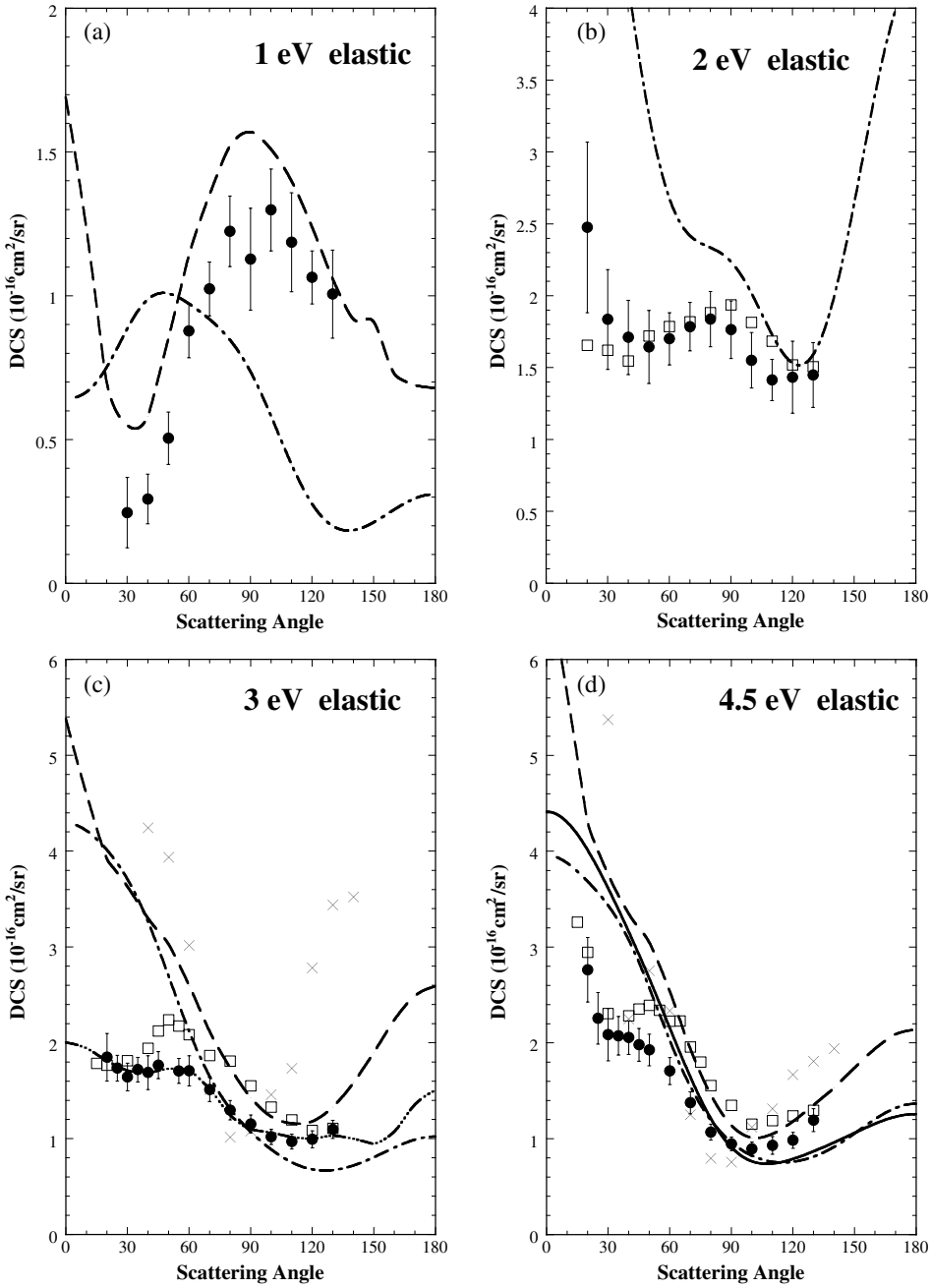

Figure 1. (a) Elastic DCS at 1 eV (in units of 10^{-16} cm^2 sr^{-1}): (●) present results—ANU, (– – –) SVIM calculation, (— · · —) Kohn calculation (see text). (b) Elastic DCS at 2 eV (in units of 10^{-16} cm^2 sr^{-1}): (●) present results—ANU, (□) present results—Sophia, (— · · —) Kohn calculation (see text). (c) Elastic DCS at 3 eV (in units of 10^{-16} cm^2 sr^{-1}): (●) present results—ANU, (□) present results—Sophia, (×) Mapstone and Newell, (— — —) SVIM calculation, (— · · —) Kohn calculation, (— · · —) MPSA fit to ANU data (see text). (d) Elastic DCS at 4.5 eV (in units of 10^{-16} cm^2 sr^{-1}): (●) present results—ANU, (□) present results—Sophia, (×) Mapstone and Newell, (– – –) SVIM calculation, (— · · —) Kohn calculation, (——) Schwinger variational calculation (see text).

structure evident, it is essentially isotropic across the angular range studied. There is also good agreement between the present results from our two laboratories, at this their lowest common energy. The Kohn variational calculation predicts a DCS which is considerably larger than experiment at forward angles but in good agreement in the region of the shallow minimum at around 120°. At 3 eV (figure 1(c)) the two data sets are once again in reasonable agreement, although the ANU cross section is smaller than that from Sophia (measured at an energy of 3.1 eV) at scattering angles between 40° and 100°. At this energy we show a comparison with the relative cross section measurement of Mapstone and Newell (1992) at an energy of 3.3 eV, and with the SVIM and Kohn cross sections, the former of these also being for the slightly higher impact energy of 3.3 eV. The data of Mapstone and Newell are not absolute so they have been normalized to the present results at an angle of 70°. The resultant cross section bears little resemblance to the present measurements and, with the normalization at mid angles, is at least a factor of 3 larger than the present measurements at angles of 30° and 130°. Neither calculation is in agreement with experiment over the entire angular range although at backward angles both give a reasonable prediction of the cross section magnitude. It is interesting to note that the structure observed in the DCS by both experiments at small scattering angles, as has been observed in many other molecules (e.g. NO, CO, N_2O—for the latter see Kitajima *et al* (2000)) at energies just above the low-energy shape resonance region, is not predicted by either calculation. Finally in this group of figures (figure 1(d)) we show the elastic DCS at an energy of 4.5 eV. At this energy we can also compare with the data of Mapstone and Newell and the SVIM, Kohn and Schwinger (Winstead and McKoy 2002) calculations. This latter calculation is an extension of the earlier work of this group (Winstead *et al* 1991) but differs from the earlier work in that it includes polarization effects. It also differs from the other Schwinger calculation (the SVIM) principally in the way in which polarization effects are treated. The cross section of Mapstone and Newell is normalized to the Sophia data at an angle of 40° and the level agreement between the measurements, particularly at larger scattering angles, is substantially better than at 3 eV. Potential problems with the lower-energy data of Mapstone and Newell were first identified by Karwasz *et al* (2001) and our results are consistent with their analysis. There is also a significant difference between the two present cross section measurements for angles larger than about 60°. The cross section from the ANU spectrometer is uniformly lower than that from Sophia by about 25%. Each of the theoretical calculations seems to reproduce the general features of the DCS, although they clearly overestimate the cross section at small angles.

In figure 2(a) the elastic DCS at an energy of 8 eV is shown. The present measurements are in good agreement with one another at forward angles but, once again, beyond about 60° there are significant differences (20–30%) in their absolute magnitudes. The measurements of Mapstone and Newell at this energy were placed on an absolute scale by normalization to an earlier Schwinger calculation of McKoy, and they are in good agreement with the present results, particularly those from the ANU. All three calculations are in good overall agreement with the experimental data, and this is particularly true for the cross section of Winstead and McKoy (2002). At 15 eV (figure 2(b)) there is once again good agreement between the three experimental results at forward angles. At larger scattering angles the ANU cross section is again smaller than that from Sophia by 20–30% but the latter is in good agreement with the measurement of Mapstone and Newell. Once again all three calculations provide a good description of the experimental results. The final comparison between the two new experiments and theory for elastic scattering comes at an energy of 20 eV (figure 2(c)) where the differences between the experiments at larger angles are similar to what we have seen at lower energies. Both experimental results are, however, smaller than all of the calculated cross sections at angles above about 20°.

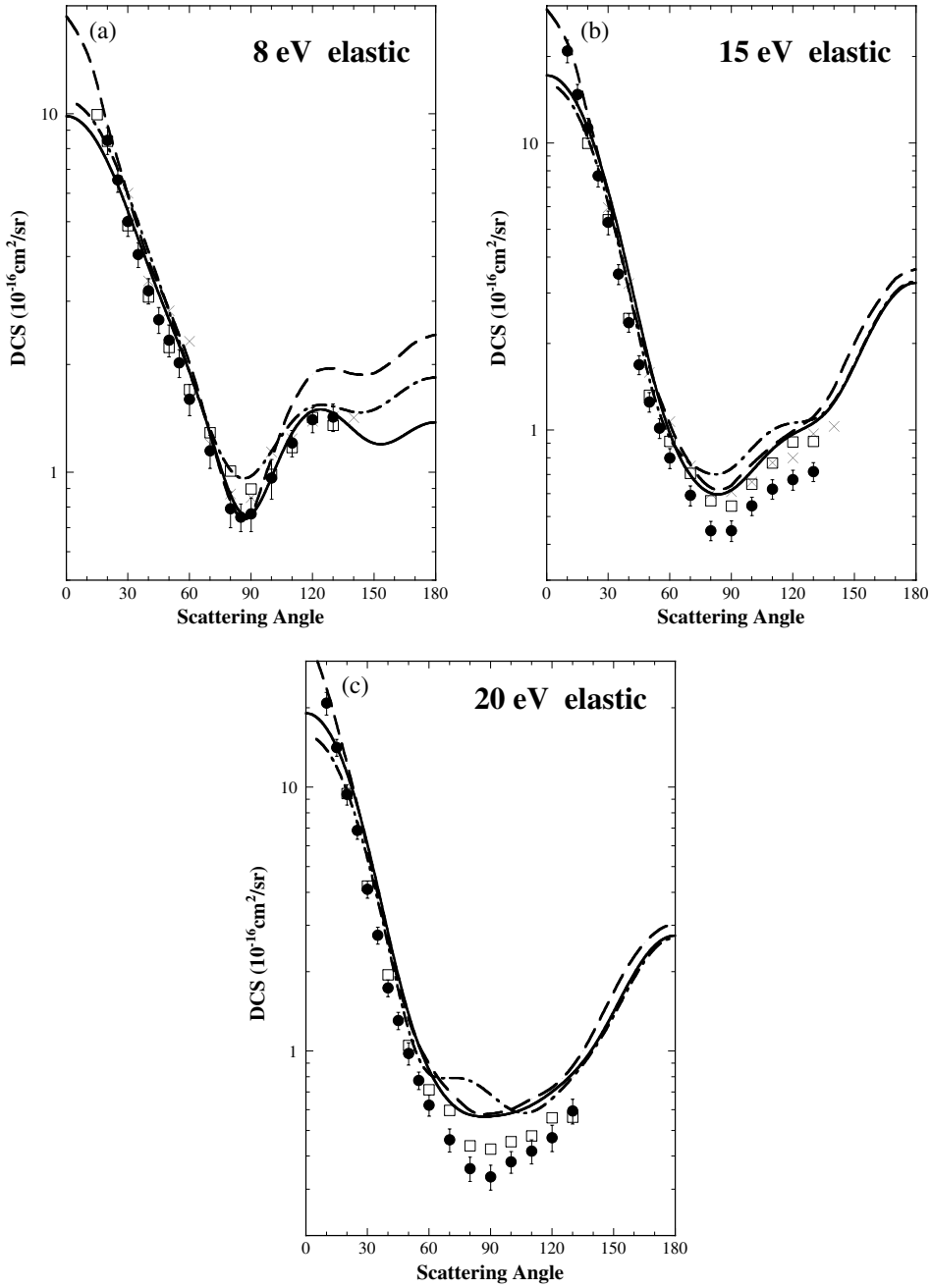

Figure 2. (a) Elastic DCS at 8 eV (in units of 10^{-16} cm^2 sr^{-1}): (●) present results—ANU, (□) present results—Sophia, (×) Mapstone and Newell, (— — —) SVIM calculation, (— · · —) Kohn calculation, (——) Schwinger variational calculation (see text). (b) Elastic DCS at 15 eV (in units of 10^{-16} cm^2 sr^{-1}): (●) present results—ANU, (□) present results—Sophia, (×) Mapstone and Newell, (– – –) SVIM calculation, (— · · —) Kohn calculation, (——) Schwinger variational calculation (see text). (c) Elastic DCS at 20 eV (in units of 10^{-16} cm^2 sr^{-1}): (●) present results—ANU, (□) present results—Sophia, (×) Mapstone and Newell, (– – –) SVIM calculation, (— · · —) Kohn calculation, (——) Schwinger variational calculation (see text).

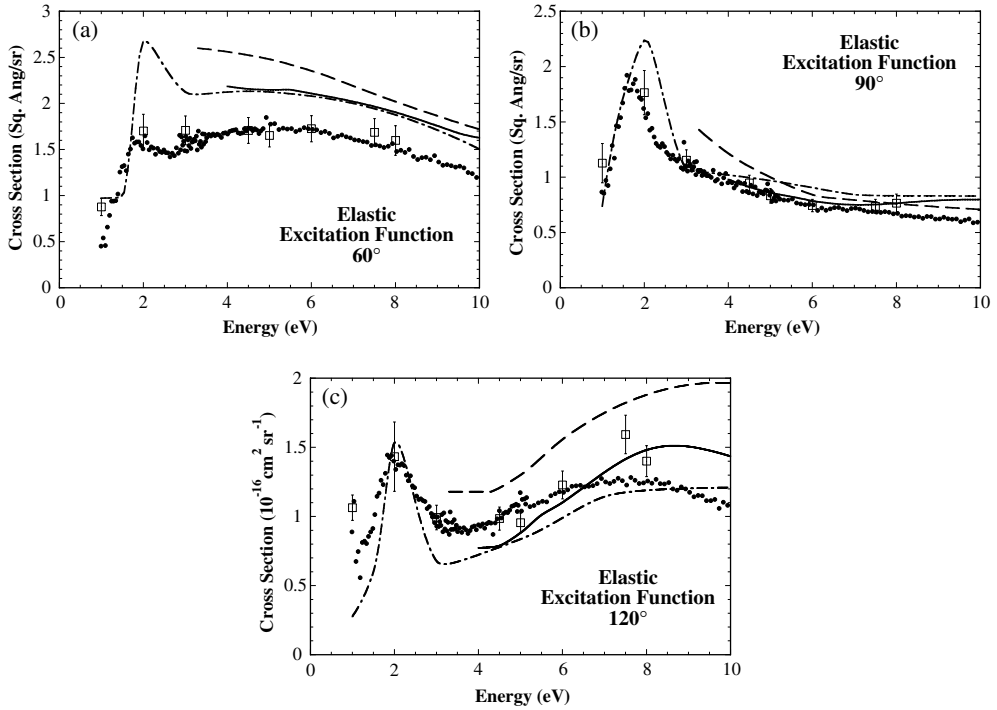

Figure 3. Absolute elastic EF (in units of 10^{-16} cm^2 sr^{-1}) for C_2H_4 between 1 and 10 eV at a scattering angle of (a) 60°, (b) 90° and (c) 120°: (●) EF measurements, (□) DCS measurements, (– – –) SVIM calculation, (— · · —) Kohn calculation, (——) Schwinger variational calculation (see text).

We next show some measurements of the energy dependence of the elastic scattering cross section (elastic EFs) at energies between 1 and 10 eV that illustrate the role of the low-lying resonances on the elastic scattering cross section. Absolute EFs at angles of 60°, 90° and 120° are given in figures 3(a)–(c). These have been measured on the ANU apparatus by measuring the ratio of elastic scattering from C_2H_4 to that of He as a function of energy. In this procedure, which has been described previously in Gibson *et al* (1996), the zoom lenses controlling both the incident and scattered beams are scanned in conjunction with the beam energy in order to optimize the transmission of the spectrometer at each energy, and the electron beam current is measured at each energy step. The absolute values are obtained by applying the relative flow technique and using the theoretical cross sections of Nesbet (1979), also calculated at each energy step.

At an angle of 60° there is evidence for the presence of the low-lying $^2B_{2g}$ shape resonance at an energy of around 1.8 eV, and also for a broad feature between 4 and 8 eV which has been classified previously as being due to an ^2A_g resonance (Walker *et al* 1978). It can also be seen that the cross sections obtained using this technique are in good agreement with those from the angular DCS measurements discussed above, which were conducted at fixed incident energies. At 90° (figure 3(b)) the lower-energy resonance is much more visible in the EF, showing as a strong peak above the direct scattering cross section with a width (FWHM) of about 700 meV. There is no evidence for the higher-lying resonance at this angle. Finally in figure 3(c) we show the EF for a scattering angle of 120°. In this case both resonances are clearly evident in

the EF, and indeed they appear to have a strong influence on the elastic cross section throughout this entire energy region. Also shown in these figures are the results from the two Schwinger calculations and the Kohn variational technique. The theory is in good general agreement with the experimental results although there are some obvious differences in absolute magnitude, particularly at 60° and 120°. The Kohn variational calculation also provides a reasonable description of the position and magnitude of the low-energy shape resonance.

The DCS data for elastic scattering have been analysed at each energy using a molecular phase shift analysis (MPSA) technique. We have derived integral cross sections (ICS) and MTCS from the present differential measurements using a generalized version of the MPSA technique of Boesten and Tanaka (1991). In this application the scattering amplitude is written as

$$f(\theta) = \frac{1}{2ik}\sum_{\ell=0}^{L}(2\ell+1)(e^{2i\delta_\ell}-1)P_\ell(\cos\theta) + \frac{1}{2ik}\sum_{\ell_>=L+1}^{\ell_{max}}(2\ell_>+1)(e^{2i\delta_{\ell_>}}-1)P_{\ell_>}(\cos\theta) \tag{1}$$

with, for $\ell > L$,

$$\tan\delta_{\ell_>} = \frac{\alpha\pi k^2}{(2\ell_>+3)(2\ell_>+1)(2\ell_>-1)}. \tag{2}$$

The DCS then follows from the relation

$$\sigma(\theta) = |f(\theta)|^2. \tag{3}$$

Here k is the wavenumber of the free electron, $P_\ell(\cos\theta)$ are the Legendre polynomials, α is the dipole polarizability of the target (=31.8 a_0^3 for C_2H_4) and δ_ℓ are the 'phase shifts' of the partial waves. Note we have annotated 'phase shifts' because electron scattering from C_2H_4 is clearly not a straightforward central potential problem. Consequently the 'phase shifts' we derive cannot be directly interpreted as corresponding to those that are familiar from the central potential scattering system. Indeed the physical meaning of our derived 'phase shifts' is unclear beyond that of being the free parameters in the functional form given by equations (1) and (3) and used in our fits. In the MPSA procedure equations (1)–(3) are fitted to the experimental DCS data by a least-squares algorithm (χ^2 minimization; see Bevington and Robinson (1990)). The 'phase shifts' for $\ell = 0$ to L are treated as the free parameters to be determined in the fit. In this work $L = 7$ was typically sufficient to give a good fit to the DCS. Note that the size factor, $N(k)$, often employed in equation (1) as an additional parameter in the approach of Boesten and Tanaka, is not utilized in our application. Similarly, their inelasticity parameter (β_ℓ) is effectively fixed here at a value of 1 for all $\ell \leqslant L$. This is equivalent to assuming the 'phase shifts' are real, whereas in general they are in fact complex. The approximation of setting $\beta_\ell = 1$ was tested thoroughly against available convergent close coupling (CCC) DCS results from Bray and colleagues, for the $1\,^1S$, $2\,^1S$ and $2\,^3P$ states of helium at energies in the range 1–30 eV. In those tests the calculated CCC DCS, for angles between 20° and 130°, in 10° increments, were fitted using our procedure and the corresponding ICS determined. In all cases the derived ICS from our analysis agreed with those calculated directly from the CCC to better than 4%. Nonetheless, even with these additional approximations, the resultant fit removes a lot of the subjectivity in the extrapolation of the measured DCS to 0° and 180°, particularly if a 'by eye' approach had to be employed. An example of the MPSA fit to the measured data for elastic scattering at 3 eV is given in figure 1(c). Having used the MPSA to obtain the angular extrapolation to 0° and 180°, the ICS and MTCS were then calculated in the usual fashion. These values can be found at the foot of each column in table 1.

The results for the integral elastic cross section are shown in figure 4(a). Here we also compare with results for the grand total cross section and with several theoretical calculations

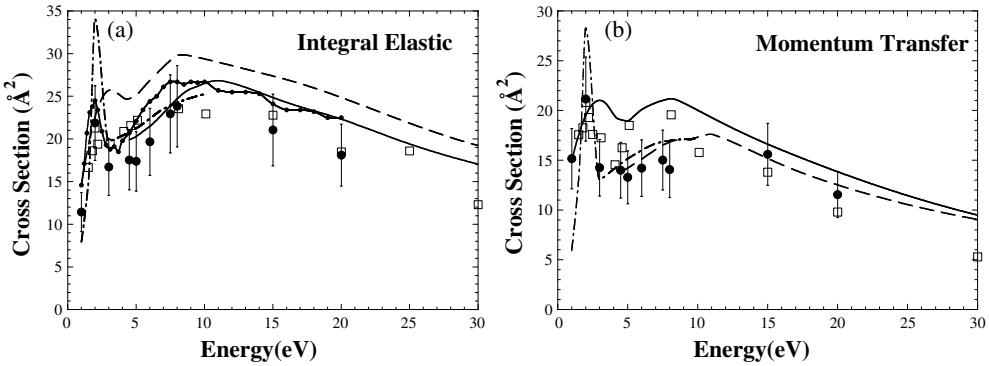

Figure 4. (a) Integral elastic cross section for C_2H_4 (in units of 10^{-16} cm^2): (●) present results—ANU, (□) present results—Sophia, (— • —) total cross section of Sueoka and Mori, (– – –) SVIM calculation, (— · · —) Kohn calculation, (——) Schwinger variational calculation (see text). (b) Elastic MTCS for C_2H_4 (in units of 10^{-16} cm^2): (●) present results—ANU, (□) present results—Sophia, (– – –) SVIM calculation, (— · · —) Kohn calculation, (——) Schwinger variational calculation (see text).

of the elastic cross section. As expected, the present ICS lie below the grand total cross section measurements of Sueoka and Mori (1986). They are also smaller in magnitude than the theoretical estimates but there is good general agreement between experiment and theory as to the overall energy dependence of the cross section, including the low-energy shape resonance. The elastic MTCS is presented in figure 4(b) and we see a similar level of good agreement between the present experiments and the theoretical calculations.

3.2. Vibrational excitation

We have investigated absolute vibrational excitation cross sections at one incident energy, 7.5 eV, where there are previous differential measurements by Walker *et al* (1978) and Mapstone *et al* (2000). The main motivation for the present measurements was to cross-check the absolute normalization of the previous data which either had relatively large uncertainties (Walker *et al*) or was normalized via a theoretical cross section (Mapstone *et al*). The present measurements are limited to that of a vibrational composite centred at an energy loss of 374 meV. A number of vibrational modes may contribute to the structure observed in our electron energy loss spectrum at this energy but the main one is believed to be the totally symmetric ν_1 mode which is strongly Raman active. The absolute DCS for the excitation of C_2H_4 at this energy loss is shown in figure 5, where it is seen to compare well with the previous measurements. The comparison with the measurement of Mapstone *et al* is the most direct as these authors also measured the cross section for a vibrational composite, with an energy resolution which was similar to the present work. Also, the small difference in magnitude between the present measurements and the higher-resolution measurements of Walker *et al* for the ν_1 mode alone, indicates that the main contributor to the composite mode excitation is the ν_1 mode. There is apparently a little additional structure in the present measurement than was observed by Walker *et al* for the ν_1 mode only. However, their additional DCS measurements for the ν_3 and ν_7 modes show evidence of weak structure and is interpreted as the manifestation of higher-order angular momentum contributions to these modes in the decay of the ^2A_g resonance. It is most likely these contributions that cause the structure in the present composite-mode DCS measurements.

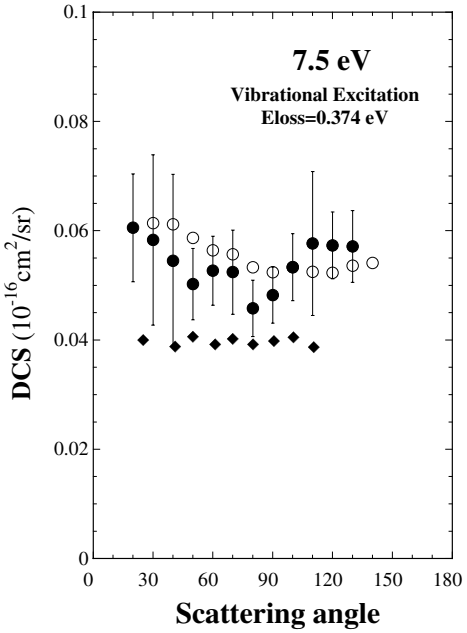

Figure 5. Absolute DCS (in units of 10^{-16} cm^2 sr^{-1}) for the excitation of a composite of vibrational modes of C_2H_4 at an energy loss of 0.374 eV: (●) present results, (○) Mapstone *et al* at 8 eV, (♦) Walker *et al* for the ν_1 mode.

It is also interesting to note that the contribution of the ^2A_g resonance to vibrational excitation appears to be significantly smaller than that to elastic scattering.

4. Conclusions

The present measurements provide the first comprehensive study of absolute elastic electron scattering from ethylene, giving a body of DCS and ICS values between 1 and 100 eV. While the data reveal some discrepancies with current scattering theory, particularly at electron energies below about 5 eV, the theoretical approaches generally provide a satisfactory account of the scattering cross sections across a reasonably broad energy range.

There are some differences (∼20–30%) between the present measurements which have been performed on different experimental apparatus, and these differences are of some significance as they lie outside the combined uncertainties of the two experiments. The origins of these differences are not yet understood. However, they do not overshadow the generally good agreement between the two experiments and, at low energies (<5 eV), this good accord highlights the discrepancies which are observed with the earlier data of Mapstone and Newell (1992).

Acknowledgments

It is a pleasure to acknowledge helpful discussions with Carl Winstead, Luiz Brescansin and Tom Rescigno and to thank them all for the provision of tabulated cross sections. Many of the collaborative aspects of this project have been supported by a grant from the Australian Research Council.

References

Bevington P R and Robinson D K 1990 *Data Reduction and Error Analysis for the Physical Sciences* (New York: McGraw-Hill)

Boesten L and Tanaka H 1991 *J. Phys. B: At. Mol. Opt. Phys.* **24** 821

Boesten L and Tanaka H 1992 *At. Data Nucl. Data Tables* **52** 25

Brescansin L M, Machado L E and Lee M-T 1998 *Phys. Rev.* A **57** 3504

Cho H, Gulley R J, Sunohara K, Kitajima M, Uhlmann L J, Tanaka H and Buckman S J 2001 *J. Phys. B: At. Mol. Opt. Phys.* **34** 1019

Floeder K, Fromme D, Raith W, Schwab A and Sinapius G 1985 *J. Phys. B: At. Mol. Phys.* **18** 3347

Gibson J C, Morgan L A, Gulley R J, Brunger M J, Bundschu C T and Buckman S J 1996 *J. Phys. B: At. Mol. Opt. Phys.* **29** 3197

Karwasz G P, Brusa R S and Zecca A 2001 *Rev. Nuovo Cimento* **24** 1

Kitajima M, Sakamoto Y, Gulley R J, Hoshino M, Gibson J C, Tanaka H and Buckman S J 2000 *J. Phys. B: At. Mol. Opt. Phys.* **33** 1687

Landolt-Börnstein 1971 *Zhalenwerte und Funktionen* vol 2, Part 1 (Berlin: Springer)

Lunt S L, Randell J, Ziesel J P, Mrotzek G and Field D 1994 *J. Phys. B: At. Mol. Opt. Phys.* **27** 1407

Mapstone B, Brunger M J and Newell W R 2000 *J. Phys. B: At. Mol. Opt. Phys.* **33** 23

Mapstone B and Newell W R 1992 *J. Phys. B: At. Mol. Opt. Phys.* **25** 491

Nesbet R K 1979 *Phys. Rev.* A **20** 58

Panajotovic R, Kitajima M, Tanaka H, Jelisavcic M, Lower J and Buckman S 2003 *Rad. Phys. Chem.* at press

Rescigno T R 2002 private communication

Schneider B I, Rescigno T N, Lengsfield B H and McCurdy C W 1991 *Phys. Rev. Lett.* **66** 2728

Sueoka O and Mori S 1986 *J. Phys. B: At. Mol. Phys.* **19** 4035

Walker I C, Stamatovic A and Wong S F 1978 *J. Chem. Phys.* **69** 5532

Winstead C, Hipes P G, Lima M A P and McKoy V 1991 *J. Chem. Phys.* **94** 5455

Winstead C and McKoy V 2002 private communication